

Determination of the best optimal estimation parameters for validation of infrared hyperspectral sounding retrievals

X. Calbet

EUMETSAT, Am Kavallerisand 31, 64295 Darmstadt, Germany
(Xavier.Calbet@eumetsat.int)

March 3, 2013

Abstract

The availability of hyperspectral infrared remote sensing instruments, like AIRS and IASI, on board of Earth observing satellites opens the possibility of obtaining high vertical resolution atmospheric profiles. We present an objective and simple technique to derive the parameters used in the optimal estimation method that retrieve atmospheric states from the spectra. The retrievals obtained in this way are optimal in the sense of providing the best possible validation statistics obtained from the difference between retrievals and a chosen calibration/validation dataset of atmospheric states. This is demonstrated analytically. To illustrate this result several real world examples using IASI retrievals fine tuned to ECMWF analyses are shown. The analytical equations obtained give further insight into the various contributions to the biases and errors of the retrievals and the consequences of using other types of fine tuning. Retrievals using IASI show an error of 0.9 to 1.9 K in temperature and below 6.5 K in humidity dew point temperature in the troposphere on the vertical radiative transfer model pressure grid (RTIASI-4.1), which has a vertical spacing between 300 and 400 m. The more accurately the calibration dataset represents the true state of the atmosphere, the better the retrievals will be when compared to the true states.

1 Introduction

Temperature and water vapor soundings from satellites has a history dating back to the early 1970s with the NIMBUS series of operational weather satellites (e.g. Wick, 1971). The next generation of instruments improved the horizontal and vertical resolution of the soundings, in particular the instruments that comprise the TOVS (TIROS Operational Vertical Sounder; Smith et al., 1979) and the more recent ATOVS (Advanced TIROS Operational Vertical Sounder; Kidwell, 1986). The latter consists of the AMSU (Advanced Microwave Sounding Unit) and HIRS (High Resolution Infrared Sounder) and provides soundings with an accuracy of about 2.0K for the temperature at 1-km vertical resolution and below 6.0K for the dewpoint temperature at 2-km vertical resolution (Li, 2000). However, in order to make further advancements, the numerical weather prediction and climate monitoring communities required improvements in both accuracy for temperature ($< 1\text{K}$) and for humidity ($< 10\%$) in the troposphere (World Meteorological Organization, 1998). It became apparent that to achieve these accuracies a new generation of instruments known now as hyperspectral infrared sounders were needed. Smith (1991) gives a detailed overview of the evolution of satellite sounding up to the hyperspectral sounders we have today. AIRS (Atmospheric InfraRed Sounder; Pagano et al. 2003; Aumann et al. 2003) and IASI (Infrared Atmospheric Sounding Interferometer; Chalon, Cayla and Diebel 2001; Blumstein et al. 2004), on board of Earth observing satellites are the prime examples of these type of instruments with a spectral coverage within the $3.62 - 15.5\mu\text{m}$ region and a spectral resolution ($\lambda/\Delta\lambda$) higher than 1000 which can achieve the required accuracies in temperature and humidity retrievals in the troposphere (Smith 1991).

There are currently three types of methods generally used to retrieve temperature and humidity profiles from these type of instruments: linear regression methods usually based on Empirical Orthogonal Functions (e.g. Smith and Woolf, 1975; Zhou, 2002), neural networks (e.g. Blackwell, 2005) and model inversion methods (Twomey, 1977), also known as Bayesian atmospheric flux inversion (Michalak, 2005), optimal estimation (Rodgers, 1976), physical retrievals (Li, 2000; Susskind, 2003). The latter type of methods can vary in several details such as the choice of measurement error covariance matrix, constraints applied, etc. Whenever one of these methods makes use of synthetic radiances generated from a radiation transfer model, some inversion parameters must be fine tuned to match the retrieval method to the real world measurements. In this paper, we will deal only with the model inversion method which is commonly known as optimal estimation (Rodgers, 2000). Its particularity is that the constraints are based on an a-priori state

of the atmosphere and its associated background covariance matrix. The same type of analytical study as the one presented here can be made on the EOF linear regression method when it is trained with synthetic data (Calbet and Schlüssel 2006) or on any of the other methods as long as they can be described analytically.

Methods to retrieve temperature and humidity profiles from these kind of instruments have been developed over the years. Modern methods can perform retrievals over clear, cloudy, land or ocean scenes (Susskind, 2003; Zhou, 2005). Despite the significant abundance of non-clear cases, the physical state parameters are better known for clear over ocean scenes, in particular surface emissivity and cloud properties. In fact, these cases provide the best retrieval statistics (e.g. Susskind 2003). Because of this, the calibration explained in this paper is preferably best performed on these cases. This fine tuning can later be extrapolated to retrieve profiles for any kind of scene. Also, to prove that the fine tuning derived here is optimal we need to verify it in practice with the best possible cases available. This is the reason why in this paper we will deal mainly with clear sky over ocean scenes.

The first and most critical tuning step is to adjust the numerical modelling of the atmosphere to the real world. This can be done by fine tuning the radiative transfer model to fit the measurements (Strow, 2006). This procedure is usually not enough to obtain un-biased retrievals and it is usually necessary to apply bias corrections to the radiances or brightness temperature (Li, 2000; Susskind, 2006). The bias corrections are usually obtained from the measurements by calculating the average of the difference between the real observed spectra and the calculated spectra obtained from some collocated calibration dataset of atmospheric states and a radiative transfer model. In a later retrieval step, measured (or modeled) spectra must be bias corrected with the above calculated average. In this paper we will provide an analytical justification to use this method and we will also show that it is optimal.

The second set of elements to be tuned in the retrieval process are the various parameters used in the optimal estimation: measurement error covariance matrix, a-priori state and a-priori error covariance matrix. For the retrieval method to work precisely we need to match with a relatively high degree of accuracy these elements of the retrievals to the real atmospheric system. The a-priori parameters are usually determined from some climatology or numerical weather model fields which are representative of the atmospheric states being retrieved. Contrary to the bias corrections, the measurement error covariance matrix is not usually derived from the measurements, but rather taken from the instrument noise and/or adding to it some estimation of the radiative transfer model error (e.g. Susskind, 2003;

Rodgers, 1990; Eyre 1990). The reason for this is to maintain the measurement error covariance as small as possible to obtain some “ideal best” retrieval, relying very much on the assumptions made and the validity of the modelling of the atmosphere. In this paper we will abandon this hypothetical concept of “ideal best” retrievals and take a more pragmatic approach. We will aim to reproduce as accurately as possible the states of the atmosphere as measured by some alternative instrument, typically either radiosondes or Numerical Weather Prediction (NWP) analyses. These measurements will be denominated calibration or validation dataset indistinctively throughout this paper. By minimizing the standard deviation between the retrievals and the validation dataset of atmospheric states we will demonstrate analytically that there exists an optimal measurement error covariance matrix for a particular validation dataset. This measurement error covariance matrix is precisely the one obtained from the difference between the real observed spectra and the calculated spectra obtained from the calibration dataset of atmospheric states and the radiative transfer model. Since this matrix will also contain representativeness and accuracy errors of the calibration dataset of atmospheric states, it will depart from an hypothetical “ideal best” measurement error. We will show that this is normally not a problem in the retrievals since it is safer to overestimate (Eyre, 1990) the measurement error of the retrievals with respect to some absolute truth, as it certainly happens with the method presented here, than to underestimate it, as it can potentially happen by using the above mentioned methods.

In the field of trace gases retrievals, Michalak et al. (2005) are also deriving the measurement error covariance matrix from the measurements themselves. The technique consists of maximizing the likelihood of the measurement covariance given a radiative transfer model, an a-priori state and a given set of measurements by applying the Bayes’ rule. The maximizing solution is quite complex analytically and it has to be solved numerically with an iterative process to obtain the measurement error covariance. The spirit of the method presented here is very similar to the one from Michalak et al. (2005) but minimizing the statistics of the retrievals with respect to the validation dataset of atmospheric states, therefore obtaining the optimal retrievals. They are optimal in the sense that they give the minimum bias and standard deviations when compared to the validation dataset. Being a simple method, the optimal measurement error covariance matrix can be derived analytically and calculated with real data in a straight forward way. The method offers an objective methodology for populating the measurement error covariance of the optimal estimation.

The fact that the solution is derived analytically gives an important insight into what elements are affecting the resulting statistics of the retrievals

when compared with the validation dataset of atmospheric states. We can even see how the retrieval error behaves when we use different measurement error covariance matrices. Other behaviors of the retrieval system could be further studied, like for example what are the consequences of using another optimal criteria different than minimizing the statistics of the retrievals, etc.

In Section 2 the method and the underlying assumptions are explained. The analytical results and proof of this method being optimal are explained in Section 3 and shown in Appendix A. The tools used to apply the method are explained in Section 4. Results of this method applied to real world data are shown in Section 5. Finally in Section 6 we discuss the method and results.

2 Best Parameter Determination Method

2.1 General Assumptions

There are some underlying assumptions when applying this method which are worth mentioning. They are directly related to the goals we are pursuing with the retrievals.

1. The ultimate goal are the retrievals themselves and to have them as accurate as possible. This also implies that we want to validate the retrievals with an alternative measurement of the state of the atmosphere.
2. We recognize that the current modelling of the atmosphere is not accurate enough to provide some “ideal best” retrievals, but rather that we will need to calibrate the whole retrieval system with some calibration dataset of atmospheric states.
3. We will assume that the scene under observation is measured only once from space, although more than one instrument or channel can be used. In this paper we will use IASI measurements. See Toohey and Strong (2007) for an interesting discussion on cross calibration of different platforms.
4. We have only one alternative type of measurement of the atmospheric state which will constitute our calibration/validation dataset. For example, in this paper we will use NWP analyses fields to calibrate and optimize the validation of the retrievals. This is in contrast to using more than one source of atmospheric information, like combining NWP and radiosonde data to fine tune and optimize the retrieval parameters.

Dealing with two different sources of atmospheric measurements for fine tuning will not be dealt with in this paper. Even so, we can still perform the exercise of validating the retrievals with another source of atmospheric information as is shown in Section 5.4 with radiosondes.

2.2 Fine Tuning and Retrieval

The method used can be divided in two steps, the fine tuning one and the retrieval proper one. These in turn can be broken down in the following substeps,

1. Tuning step.
 - (a) In the tuning step the measurements, radiances or brightness temperature, from the hyperspectral instrument are obtained. These will be referred to as observations (OBS).
 - (b) The next step is to find the co-located calibration dataset of the atmospheric state vector corresponding to the same scene as the IASI observation. We then calculate the spectra corresponding to this atmospheric state vector using a radiative transfer model. These will be referred to as calculations (CALC).
 - (c) We then calculate the difference between observations and calculations (OBS - CALC) for many different scenes.
 - (d) The last step is to get the statistics of this collection of OBS - CALC. In particular the mean (bias) and the covariance matrix.
 - (e) Optimal estimation is designed to work with data that has Gaussian noise. This requirement has to be fulfilled by the OBS-CALC difference. This working hypothesis should be verified by checking the OBS-CALC histograms for each channel or measurement.
2. Retrieval step.
 - (a) In the retrieval step the measured radiances or brightness temperatures are corrected with the bias calculated in the fine tuning step.
 - (b) We then use the OBS-CALC covariance obtained in the fine tuning step directly as the measurement error covariance matrix of the optimal estimation.

- (c) The background state vector and its covariance matrix can be calculated from any source as long as their statistics are similar to the ones from the real atmosphere. In this particular example they have been obtained from climatology.

3 Best parameter determination for the optimal estimation

3.1 Bias corrections

In Appendix A we give the analytical proof that the fine tuning method described here is the optimal one. It is derived for the linear method but can also be applied to the non-linear case if the first guess is close enough to the final result.

The biases in the retrievals are given by Eq. 18, which we replicate here,

$$\begin{aligned} \overline{x_R - x_v} &= \left[K^T S_\epsilon^{-1} K + S_a^{-1} \right]^{-1} \cdot \\ &\left[K^T S_\epsilon^{-1} (\overline{y_o - y_c}) + S_a^{-1} (\overline{x_a - x_v}) \right], \end{aligned} \quad (1)$$

where x_R is the retrieved atmospheric state, x_v is the atmospheric state from the calibration or validation dataset, K is the Jacobian from the radiative transfer, S_a is the background covariance matrix, S_ϵ is the measurement error covariance matrix, y_o is the observed (OBS) spectrum, y_c is the calculated (CALC) spectrum and x_a is the background a-priori atmospheric state. We can see from this expression that the bias comes from two sources. The first source is the OBS - CALC bias in the spectra $(\overline{y_o - y_c})$. The second one comes from the difference between the background a-priori and the validation dataset atmospheric state. The latter error should be small if the information content of the radiance spectra is high as is the case for IASI. In order to eliminate these biases in the retrievals, the spectral measurements should be bias corrected according to Eq. 19:

$$\overline{y_c} = \overline{y_o}, \quad (2)$$

which is effectively an OBS-CALC bias correction. Also the a-priori state, which is a constant in the retrievals, should match the calibration dataset states average (Eq. 20),

$$x_a = \overline{x_v}. \quad (3)$$

3.2 Measurement and background error covariances

In an ideal or simulated world the measurement error covariance matrix, $S_{\epsilon,i}$, is quite accurately defined as

$$S_{\epsilon,i} = \overline{(y_i - F_p(x_t))(y_i - F_p(x_t))^T}, \quad (4)$$

where y_i is an idealised instrument spectrum, F_p represents a perfect radiative transfer model and x_t is the true atmospheric state of the atmosphere. However, in the real world the instrument does not behave ideally, the radiative transfer model is not perfect and the true atmospheric state can only be approximated by measurements. This in turn implies that there is no practical way to derive the ideal $S_{\epsilon,i}$. A practical alternative solution is to estimate it from simultaneous measurements of the atmospheric state and spectra,

$$S_\epsilon = \overline{(y_o - F(x_v))(y_o - F(x_v))^T}, \quad (5)$$

where y_o is the observed spectrum, F represents the radiative model used and x_v is the measurement of the state of the atmosphere. Obviously, the better each of the components that go into this equation are, the better the approximation of $S_{\epsilon,i}$ will be. Hopefully the instrument should be well behaved, the radiative transfer model should reproduce the radiation properly and the measured atmospheric states should be as representative of the true state as possible.

In what follows we will show that this latter S_ϵ is actually the one that minimizes the errors of the retrievals when compared to the validation dataset. For practical purposes, this value is a good estimation of the ideal covariance, $S_{\epsilon,i}$, as will be shown in later sections with real world examples and by showing below that it is better to overestimate the measurement errors than to underestimate them in the retrievals.

The covariance of the retrieval error is shown in Eq. 22. To see what effect the different values of the measurement error has on a particular retrieval system, we can simplify the expression to just one measurement and one retrieved variable. This expression will not show in full detail how the actual retrieval with many variables behaves, and it is just illustrative,

$$\text{Cov}(x_R - x_v) = \frac{K^2 S_\epsilon^{-2} \overline{(y_o - y_c)^2} + S_a^{-2} \overline{(x_a - x_v)^2}}{(K^2 S_\epsilon^{-1} + S_a^{-1})^2}. \quad (6)$$

We can now plot the retrieval error as a function of S_ϵ for a given set of parameters. This is shown in Fig. 1. We can see clearly that the retrieval error increases much more rapidly when we underestimate the measurement

error than when we overestimate it. Assuming, just for this argument, that x_v is actually the absolute true state of the atmosphere and not a calibration dataset as in the rest of this paper, we can see that for practical purposes it is “safer” to overestimate the measurement error than to underestimate it.

The measurement error covariance matrix, S_ϵ , that minimizes the errors of the retrievals with respect to the validation dataset is found analytically to be (Eq. 26),

$$S_\epsilon = \overline{(y_o - y_c)(y_o - y_c)^T}, \quad (7)$$

which is exactly the OBS–CALC covariance matrix. To minimize the resulting retrieval errors, the a-priori covariance matrix, S_a , should satisfy (Eq. 27),

$$S_a = \overline{(x_a - x_v)(x_a - x_v)^T}. \quad (8)$$

This expression, together with Eq. 3, basically states that the a-priori covariance matrix should match the covariance matrix of the validation atmospheric states.

One important aspect of this analytical proof is that it can be easily modified to be used with other retrieval methods or even for validation parameters other than the average or standard deviation.

4 Practical Example

4.1 IASI Infrared Hyperspectral Measurements

The real world measurements come from the IASI instrument. IASI is a hyperspectral resolution infrared sounder on board of the polar orbiting series of Metop satellites that forms the EUMETSAT Polar System (EPS). Metop-A, the first of three satellites of the series was launched successfully on 19 October 2006, from the Baikonur Cosmodrome in Kazakhstan. IASI is a Michelson interferometer measuring between 3.62 and 15.5 microns with a spectral resolution of 0.5 cm^{-1} after apodisation. The spatial resolution is of 12 km at nadir.

4.2 Scene Selection

The scenes observed by IASI were selected for the fine tuning and retrieval step as clear sky over ocean at nighttime with latitudes equatorward of 50° . The reason for this is to keep to a minimum unknown effects which might show up, like for example, unknown surface emissivity over land, cloud properties, etc. The selection criteria to declare a certain scene cloudy or clear in the fine tuning is very critical. If a small percentage of the scenes are

cloud contaminated, this will lead to a bigger than desired bias in the final validation of the retrievals. In this paper the clear scenes selection method is the one followed by Lutz (2002, 2003) and is shown tabulated in Table 1. A total of 5308 scenes have been selected around midnight and noon on the days of 10, 11, 17, 18, 19, 27, 28 and 29 of April 2007. They were selected plus or minus one hour from midnight or noon to have an NWP analysis field close enough in time to the IASI observations. This sample was split in two, a first one of 5042 scenes to calculate the fine tuning coefficients and the rest 266 to be validated against NWP analyses fields. Although the scenes used to validate the retrievals are also clear sky over ocean ones, the same fine tuning could be used on any other type of scene. An example of this is shown in Section 5.4 where the retrievals are compared with co-located radiosondes.

4.3 Radiative Transfer Model

The radiative transfer model used is RTIASI 4.1 (Matricardi and Saunders 1999). This fast model provides both direct radiances or brightness temperatures for each IASI channel and their corresponding Jacobians. RTIASI also has a built-in model of surface emissivity which we have used in practice.

4.4 Optimal Estimation Retrievals

The retrieval method used is the non-linear optimal estimation one as explained in Rodgers (2000). The technique is applied in brightness temperature space. One of the pre-requisites to apply this method is that the errors are Gaussian. Although the instrument error is Gaussian only in radiance space, the global error covariance matrix from OBS-CALC in brightness temperature space is in fact also Gaussian. Indeed, since the OBS-CALC error covariance matrix includes, besides instrument error, also radiative model errors and NWP errors, the overall effect is a Gaussian error in brightness temperature space. This can be verified in Fig. 2 for channel 3577 (1539 cm^{-1}) where the histogram of the OBS-CALC brightness temperature has been plotted. As a counter-example and for illustrative purposes, we also show the histogram for channel 5800 (2094.75 cm^{-1}) in Fig. 3, which clearly deviates from a Gaussian function. This anomaly comes from an incorrect CO input profile to the radiative transfer model. To solve this problem we have to either discard this channel, which is the solution adopted in this paper, or try to introduce a more realistic CO profile.

Optimal estimation retrievals are performed on the temperature and water vapor profiles and skin temperature. First guess estimates come from

a previous EOF linear regression retrieval (Calbet and Schlüssel, 2006) of ozone, temperature and water vapor profiles and skin temperature.

The channels used in the retrievals are the ones with wavenumbers smaller than 1900 cm^{-1} , except the ones on the ozone band. The reasons for avoiding the shortwavelength region is that it is difficult to model daytime radiation effects, the instrument noise is high and there are absorption lines of some trace gases from which the atmospheric profiles are difficult to know (e.g. CO). The ozone band is not used because the ozone profile is not retrieved in the optimal estimation.

Brightness temperatures are bias corrected with the OBS-CALC obtained from the fine tuning step. They are then used by the optimal estimation retrieval.

The measurement error covariance matrix of the optimal estimation is the square of the standard deviation of OBS-CALC. Although the optimal error covariance matrix is actually the full OBS-CALC covariance matrix (Eq. 26), it has been verified by our own experience that only the diagonal (i.e. square of the standard deviation) is actually needed in these particular retrieval exercises. This slightly simplifies the procedure.

The atmospheric state vectors used to calculate the a-priori parameters (a-priori state vector and a-priori covariance matrix) are a modified subset of the Chevallier profiles (Chevallier 2002). These profiles constitute a representative sample of the atmosphere obtained from the 40-year re-analysis project of the European Centre for Medium-Range Weather Forecasts (ECMWF).

The non-linear optimal estimation method is solved iteratively using a minimization Levenberg-Marquardt algorithm. The iterations are finished when the cost function does not decrease significantly anymore. Note that a consequence of this is finalizing the retrievals with brightness temperature residuals well below the $1 - \sigma$ level of the measurement error covariance matrix, S_ϵ . See Section 6 for a more in depth discussion.

4.5 Calibration/Validation Dataset of Atmospheric States

The reference states of the atmosphere will be the NWP analyses from ECMWF. They are co-located by choosing the atmospheric profile of the nearest grid point of the ECMWF analysis to the IASI field of view. They also are at most only one hour apart from the IASI measurement.

4.6 Instrument Noise

Instrument noise does not have a Gaussian behavior in brightness temperature space, which is what is required by optimal estimation. Nevertheless, for the purpose of comparing with the optimal error covariance matrix (OBS-CALC), retrievals were done using instrument noise as the sole contribution to the measurement error covariance matrix. In these cases, brightness temperature instrument noise was calculated based on its measured brightness temperature for each IASI field of view.

5 Practical Example Results

5.1 Best Parameter Determination Method Results

The OBS-CALC statistics for the 5042 profiles are shown in Fig. 4 and 5. Fig. 4 shows the bias for each of the IASI wavelengths. The standard deviation of OBS-CALC as a function of IASI wavelength is shown in Fig. 5. For comparison purposes, the instrument noise in brightness temperature space for one randomly chosen IASI spectrum is also shown in Fig. 5. We can see how the total error in some regions is much higher than the instrument noise. In those particular channels where this is the case, the error contribution from the radiative transfer modelling or the representativeness of ECMWF analyses is much higher than the instrument noise. Note that since we are stopping the iterations of the optimal estimation algorithm when the cost function does not descend significantly, the final brightness temperature residuals are well below the values of the measurement error covariance matrix, S_e . See Section 6 for a more in depth discussion.

5.2 Effects of Different Measurement Error Covariance Matrices

In order to illustrate that the OBS-CALC covariance matrix is effectively the optimum one to use for the retrievals, three different error covariance matrices have been applied: the optimum one (OBS-CALC), a constant standard deviation of 2K and using only the instrument noise. The retrieval technique is the optimal estimation explained in Section 2 for all three experiments. Retrievals were made on the 266 measured IASI fields of view (which are independent of the 5042 scenes used for fine tuning). In this case non-polar, clear air, nighttime over the ocean retrievals were performed (see Section 4.2).

A comparison of all three methods (OBS-CALC, 2K and instrument noise as measurement error covariance matrices) can be seen in Fig. 6. As was expected, optimum covariance matrix (OBS-CALC) offers the best retrievals within the statistical noise of the comparison.

5.3 Statistics and Examples of Optimum Retrievals

A few examples of retrievals on non-polar, nighttime, clear sky, over the ocean scenes using the optimal error covariance matrix are shown. In Fig. 7 a typical IASI retrieval is shown together with the co-located ECMWF atmospheric profile. There is a low level inversion that is clearly retrieved in this example. Also the humidity profile is similar to the ECMWF analysis. In Fig. 8 we have a flatter temperature profile, which is also relatively well retrieved, as well as the humidity profile. In Fig. 9 we see how a strong mid level inversion is also reproduced by the retrieval even with high humidity at lower levels. In Fig. 10 a humidity maximum is well reproduced, this profile also has a strong inversion near the surface.

The global statistics of these 266 cases when using the optimal error covariance matrix is shown in Fig. 6 as a solid line (OBS-CALC). The IASI retrieval accuracy is between 0.9 and 1.9 K in temperature and below 6.5 K in humidity dew point temperature in the troposphere. Note that these statistics have been computed directly on RTIASI-4.1 pressure level grids without smoothing with the averaging kernels. This implies a vertical spacing between levels from 300 to 400 m in the troposphere.

5.4 Comparison with Radiosondes

Although the retrieval parameters have been fine tuned to ECMWF analyses, they also compare well with co-located radiosondes. In Fig. 11, 12 and 13 we show three IASI retrievals together with their co-located radiosondes launched five minutes before overpass time from campaign data obtained at Lindenberg. They were performed in clear sky situations at night and daytime. It can be seen that the retrievals reproduce particular interesting features of the atmosphere like low level temperature inversions, levels of maximum humidity and the tropopause. For illustrative purposes, the retrieval, sonde, first guess (EOF retrieval) and background state for the first of these examples is shown in Fig. 14.

6 Discussion

It is normally the case that the radiative transfer modelling of the atmosphere does not coincide exactly with the observed infrared spectrum. Although these differences may not seem to be very high, they are big enough to degrade the retrievals significantly. They can be caused by several reasons like not knowing the exact concentration of trace gases, erroneous line shapes in the radiative transfer model or non-perfect atmospheric states, just to name a few. There are usually two ways to correct for this error. The first one of them is to model the atmosphere better by either improving the radiative transfer model or by using a more realistic atmospheric state vector, like for example improving trace gases profiles. The second is to bias correct the observed radiances or brightness temperatures to match them to the radiative transfer model ones.

Usually the errors when validating the retrievals are assumed to come from three different sources (Rodgers 1990): instrument errors, radiative transfer model errors and inaccuracies in the representativeness of the calibration dataset state vectors (NWP analyses in our case). It is usually not simple to disentangle each one of these sources of errors in the retrievals. In this paper we have not tried to achieve this, but rather obtain the best possible parameters (biases, error covariance matrix and background properties) to achieve the optimal retrievals when validated with the validation dataset (NWP analyses is the example shown here). In this way, we deal with all the errors at once. This will make the method simple but at the same time powerful by providing the best possible retrievals when compared with one single source of validation dataset of atmospheric states. The price we have to pay is that the retrievals are not the best when compared with some “ideal” absolute reality of the atmosphere because we will be overestimating the measurement error by including an undesired source of error, the one from NWP analyses in this case. In particular, by using more conservative values for the measurement error covariance matrix the potential high vertical resolution of IASI retrievals might be compromised. It is clear that this method will be useful when the errors of the calibration dataset of atmospheric states compared to the absolute real ones are small enough for our purposes, as could be the case here with temperature and water vapor profiles coming from NWP analyses. In any case, as we saw in Fig. 1, it is generally safer to overestimate the measurement error, as we are doing with this method, than to underestimate it.

Note that we are using a calibration and validation dataset that does not represent the true atmospheric states perfectly (ECMWF analyses), which in turn gives what could be regarded as an oversized measurement error

covariance matrix as shown in Fig. 5. Despite of this, the retrievals do not seem to be extremely penalised in the vertical resolution with respect to what could be expected. This can be seen in Fig. 11, where a very low level temperature inversion is correctly reproduced. The reason for this is that we are stopping the iterations of the optimal estimation algorithm when the cost function does not descend significantly, which in practice means that the final brightness temperature residuals of the spectra are usually well below the values of the measurement error covariance matrix, S_e . More than the absolute values of S_e , the important parameters to be considered here are the relative amounts within the S_e matrix, which is what effectively goes into the cost function in the optimal estimation.

One drawback of this technique is that we can only use one source of atmospheric knowledge as the calibration state vector. It would be advantageous to extend this technique in such a way that more than one source of measurements could be used, for example, using NWP analyses and radiosondes at the same time.

A direct consequence of the analytical solution is that there is one and only one measurement error covariance matrix that is the optimal one for the validation dataset. If this covariance is modified to better match some other validation dataset or because we feel a lower value would work better for the “real” atmospheric states, we will have to settle with a degradation of the retrieval statistics with respect to the first validation dataset.

The retrievals would be even closer to the real atmospheric states if we used a better calibration dataset, like for example radiosondes. Unfortunately, it is difficult to obtain IASI co-located radiondes and there are not enough of them to make a statistically significant sample.

This method is the optimal one in the sense of providing the smallest bias and standard deviation in the validation of the retrievals. Other parameters different than these two could be devised to characterize the goodness of the retrievals. In this case, the analytical study could be modified to use these new parameters.

The method has been designed to make optimal retrievals. It remains to be seen whether this same or other kind of similar analytical study would also be useful for assimilation in NWP models. In this case, the processing chain is much longer and does not stop in the retrievals but extends much further up to the forecasts.

A Analytical Proof of the Best Parameter Determination Method

In this appendix we prove that the optimal bias corrections and error covariance matrix to be used in the retrievals are the OBS -CALC mean and covariance. We will show this for the linearized forward radiative transfer model.

The retrieval method consists in minimizing a cost function, J , with respect to x' . The cost function can be explicitly written as,

$$J = (y' - F(x'))^T S_\epsilon^{-1} (y' - F(x')) + (x' - x'_a)^T S_a^{-1} (x' - x'_a). \quad (9)$$

Here we have used the usual matrix notation similar to that from Rodgers (2000), being x' the atmospheric state, F the forward model, y' the hyperspectral measurements, S_ϵ the measurement error covariance matrix used in the retrieval, S_a the a-priori covariance matrix and x'_a the a-priori atmospheric state.

This complex non-linear problem is usually linearized by expanding the forward model into a Fourier series around a reference point x'_* , which in general will be different from the a-priori background state x'_a ,

$$y' \simeq y'_* + K(x' - x'_*), \quad (10)$$

where K is the Jacobian of the forward model F . We will define x and y as the departures of the atmospheric states and measurements from the reference point x'_* and y'_* respectively,

$$y \equiv y' - y'_*, \quad (11)$$

$$x \equiv x' - x'_*. \quad (12)$$

After the linearisation the cost function becomes,

$$J = (y - Kx)^T S_\epsilon^{-1} (y - Kx) + (x - x_a)^T S_a^{-1} (x - x_a). \quad (13)$$

In the retrieval process we try to minimize this function by making its derivative equal to zero,

$$\frac{\partial J}{\partial x} = -K^T S_\epsilon^{-1} (y - Kx) + S_a^{-1} (x - x_a) + [\]^T, \quad (14)$$

where $[\]^T$ denotes the transpose of the rest of the right hand side of the equation. Solving for x we obtain the familiar retrieval expression,

$$x_R = \left(K^T S_\epsilon^{-1} K + S_a^{-1}\right)^{-1} \left(K^T S_\epsilon^{-1} y_o + S_a^{-1} x_a\right), \quad (15)$$

where x_R stands for the retrieved atmospheric state and we have substituted y_o for y to stress that this is the observed spectrum. The reason for this is to differentiate this spectrum from the calculated one, y_c . The latter is obtained by applying the radiative transfer model (K) to the calibration/validation dataset of atmospheric states, x_v .

We now proceed to calculate the bias of the retrievals by comparing with the validation dataset state of the atmosphere (NWP analyses for example), x_v ,

$$x_R - x_v = \left(K^T S_\epsilon^{-1} K + S_a^{-1}\right)^{-1} \left(K^T S_\epsilon^{-1} y_o + S_a^{-1} x_a\right) - x_v. \quad (16)$$

If we now multiply the x_v term by $(K^T S_\epsilon^{-1} K + S_a^{-1})^{-1}(K^T S_\epsilon^{-1} K + S_a^{-1})$, rearranging terms and taking into account that Kx_v is what we have called the calculated spectrum, y_c , we obtain,

$$x_R - x_v = \left[K^T S_\epsilon^{-1} K + S_a^{-1}\right]^{-1} \cdot \left[K^T S_\epsilon^{-1} (y_o - y_c) + S_a^{-1} (x_a - x_v)\right]. \quad (17)$$

By taking the expected value we obtain the final expression for the bias,

$$\overline{x_R - x_v} = \left[K^T S_\epsilon^{-1} K + S_a^{-1}\right]^{-1} \cdot \left[K^T S_\epsilon^{-1} (\overline{y_o - y_c}) + S_a^{-1} (\overline{x_a - x_v})\right]. \quad (18)$$

We can see from this expression that the bias comes from two sources. The first source is the OBS - CALC bias in the spectra $(\overline{y_o - y_c})$. The second one comes from the difference between the background a-priori and the calibration atmospheric state. In order to minimize the bias in the retrievals we should bias correct the observations with the OBS - CALC average, such that in the end,

$$\overline{y_c} = \overline{y_o}. \quad (19)$$

Also the background state should be equal to the average atmospheric states being retrieved

$$x_a = \overline{x_v}. \quad (20)$$

The error of the retrievals can be measured with the covariance between the retrieved and the validation atmospheric profiles,

$$\text{Cov}(x_R - x_v) = (x_R - x_v)(x_R - x_v)^T. \quad (21)$$

If we now include the atmospheric profile difference from Eq. 17 we obtain,

$$\begin{aligned} \text{Cov}(x_R - x_v) = & \left[K^T S_\epsilon^{-1} K + S_a^{-1} \right]^{-1} \cdot \\ & \left[K^T S_\epsilon^{-1} (y_o - y_c) + S_a^{-1} (x_a - x_v) \right] \cdot \\ & \left[(y_o - y_c)^T S_\epsilon^{-1} K + (x_a - x_v)^T S_a^{-1} \right] \cdot \\ & \left[K^T S_\epsilon^{-1} K + S_a^{-1} \right]^{-1}. \end{aligned} \quad (22)$$

The optimal retrieval parameters, S_ϵ^{-1} , S_a^{-1} and x_a can be calculated by taking the derivative of this covariance with respect to S_ϵ^{-1} and making it equal to zero,

$$\begin{aligned} \frac{\partial \text{Cov}(x_R - x_v)}{\partial S_\epsilon^{-1}} = & \left[K^T S_\epsilon^{-1} K + S_a^{-1} \right]^{-1} K^T \otimes K \left[K^T S_\epsilon^{-1} K + S_a^{-1} \right]^{-1} \cdot \\ & \left[K^T S_\epsilon^{-1} (y_o - y_c) + S_a^{-1} (x_a - x_v) \right] \cdot \\ & \left[(y_o - y_c)^T S_\epsilon^{-1} K + (x_a - x_v)^T \right] \cdot \\ & \left[K^T S_\epsilon^{-1} K + S_a^{-1} \right]^{-1} \\ & + \\ & \left[K^T S_\epsilon^{-1} K + S_a^{-1} \right]^{-1} \\ & K^T \otimes [y_o - y_c] \\ & \left[(y_o - y_c)^T S_\epsilon^{-1} K + (x_a - x_v)^T \right] \cdot \\ & \left[K^T S_\epsilon^{-1} K + S_a^{-1} \right]^{-1} \\ & + [\]^T, \end{aligned} \quad (23)$$

where $[]^T$ denotes the transpose of the rest of the right hand side of the equation and the symbol \otimes represents the tensor product of two matrices in the sense that each element of the four dimensional tensor product is,

$$(A \otimes B)_{i,j,k,l} = A_{i,k} B_{l,j}. \quad (24)$$

Note that the since the covariance matrices are symmetric, $[S_\epsilon^{-1}]^T = S_\epsilon^{-1}$. The same applies for S_a^{-1} .

Rearranging terms and averaging over many cases we are left with,

$$\begin{aligned} \frac{\partial \overline{\text{Cov}(x_R - x_v)}}{\partial S_\epsilon^{-1}} = & \left[K^T S_\epsilon^{-1} K + S_a^{-1} \right]^{-1} K^T \otimes \{ \\ & -K \left[K^T S_\epsilon^{-1} K + S_a^{-1} \right]^{-1} K^T S_\epsilon^{-1} \cdot \\ & \overline{(y_o - y_c)(y_o - y_c)^T S_\epsilon^{-1} K} \\ & + \overline{(y_o - y_c)(y_o - y_c)^T S_\epsilon^{-1} K} \\ & -K \left[K^T S_\epsilon^{-1} K + S_a^{-1} \right]^{-1} K^T S_\epsilon^{-1} \overline{(y_o - y_c)(x_a - x_v)^T S_a^{-1}} \\ & -K \left[K^T S_\epsilon^{-1} K + S_a^{-1} \right]^{-1} S_a^{-1} \overline{(x_a - x_v)(y_o - y_c)^T S_\epsilon^{-1} K} \\ & -K \left[K^T S_\epsilon^{-1} K + S_a^{-1} \right]^{-1} S_a^{-1} \overline{(x_a - x_v)(x_a - x_v)^T S_a^{-1}} \\ & + \overline{(y_o - y_c)(x_a - x_v)^T S_a^{-1}} \\ & \} \left[K^T S_\epsilon^{-1} K + S_a^{-1} \right]^{-1} \\ & + []^T. \end{aligned} \quad (25)$$

We will now show that this derivative is zero if we set,

$$S_\epsilon = \overline{(y_o - y_c)(y_o - y_c)^T} \quad (26)$$

$$S_a = \overline{(x_a - x_v)(x_a - x_v)^T}. \quad (27)$$

Introducing Eqs. 26 and 27 into Eq. 25 we can certify that all terms including only x 's or y 's of Eq. 25 vanish, leaving only x and y cross-product terms.

Let us now analyze the cross-product term and show that it is also zero,

$$\overline{(y_o - y_c)(x_a - x_v)^T} = \overline{(y_o - y_c)} x_a^T - \overline{y_o x_v^T} + \overline{y_c x_v^T} \quad (28)$$

The first term of the right hand side is zero when we apply the bias corrections from Eq. 19. If the forward model, F , reproduces well enough the properties of the real atmosphere, the calculated spectra should have similar statistical properties as the observed one in the sense that their cross-covariances with the validation atmospheric states should be similar,

$$\overline{y_o x_v^T} \approx \overline{y_c x_v^T}, \quad (29)$$

which implies that the last two terms of the right hand side of Eq. 28 are also approximately zero.

This concludes the proof obtaining as results Eqs. 19, 20, 26 and 27. Using these solutions we can also calculate the final error retrieval covariance matrix to obtain,

$$\text{Cov}(x_R - x_v) = \left[K^T S_\epsilon^{-1} K + S_a^{-1} \right]^{-1}, \quad (30)$$

which is the usual accepted expression (Rodgers 2000).

References

- [aumann2003] Aumann, H.H. et al. (2003), AIRS/AMSU/HSB on the Aqua mission: Design, science objectives, data products, and processing systems, *IEEE Trans. Geosci. Remote Sens.*, 41, 253-264.
- [blackwell2005] Blackwell, W.J. (2005), A neural-network technique for the retrieval of atmospheric temperature and moisture profiles from high spectral resolution sounding data, *IEEE Trans. Geosci. Remote Sens.*, 43, 2535-2546.
- [blumstein2004] Blumstein, D., G. Chalon, T. Carlier, C. Buil, P. Hébert, T. Maciaszek, G. Ponce, T. Phulpin, B. Tournier, and D. Siméoni (2004), IASI instrument technical overview and measured performances, *SPIE Conference*, Denver (Co), August 2004 SPIE 2004-5543-22.
- [calbet2006] Calbet, X. and P. Schlüssel (2006), Technical note: Analytical estimation of the optimal parameters for the EOF retrievals of the IASI Level 2 Product Processing Facility and its application using AIRS and ECMWF data, *Atmos. Chem. Phys.*, 6, 831846.
- [chalon2001] Chalon G., F. Cayla and D. Diebel (2001), IASI: An Advanced Sounder for Operational Meteorology, Proceedings of the 52nd Congress of IAF, Toulouse France, 1-5 Oct. 2001.

- [chevallier2002] Chevallier, F. (2002), Sampled databases of 60-level atmospheric profiles from the ECMWF analyses, NWP SAF Doc. No. NWPSAF-EC-TR-004.
- [eyre1990] Eyre, J.R. (1990), The information content of data from satellite sounding systems: a simulation study, *Q. J. R. Meteorol. Soc.*, *116*, 401-434.
- [kidwell1986] Kidwell, K.B. (1986), NOAA Polar Orbiter Data User's Guide, NOAA/NESDIS Satellite Data Services Div., Washington D.C.
- [li2000] Jun Li, J., W. W. Wolf, W.P. Menzel, W. Zhang, H. Huang and T.H. Achtor (2000), Global Soundings of the Atmosphere from ATOVS Measurements: The Algorithm and Validation, *Journal of Applied Meteorology*, *39*, 1248-1268.
- [lutz2002] Lutz, H.J. (2002), Scenes Analysis from MODIS and Meteosat Observations, Proceedings of the 2002 EUMETSAT Meteorological Satellite Data Users' Conference, 8.
- [lutz2003] Lutz, H.J. et al. (2003), Comparison of a Split-window and a Multi-spectral Cloud Classification for MODIS Observations, *Journal of the Meteorological Society of Japan*, *81*(3), 623-631.
- [matricardi1999] Matricardi M. and R. W. Saunders, 1999, M. Matricardi and R.W. Saunders, Fast radiative transfer model for simulation of infrared atmospheric sounding Interferometer radiances, *Appl. Opt.*, *38*, 5679-5691.
- [michalak2005] Michalak, A.M., A. Hirsch, L. Bruhwiler, K.R. Gurney, W. Peters, P.P. Tans, Maximum likelihood estimation of covariance parameters for Bayesian atmospheric trace gas surface flux inversions, *J. Geo. Res.*, *110*, D24107.
- [pagano2003] Pagano, T.S., H.H. Aumann, D.E. Hagan, and K. Overoye (2003), Pre-launch and in-flight radiometric calibration of the Atmospheric Infrared Sounder (AIRS), *IEEE Trans. Geosci. Remote Sens.*, *41*, 265-273.
- [rogers1976] Rodgers, C.D. (1976), Retrieval of atmospheric temperature and composition from remote measurements of thermal radiation, *Rev. Geo. and Space Phys.*, *14*, 609-624.
- [rogers1990] Rodgers, C.D. (1990), Characterization and error analysis of profiles retrieved from remote sensing measurements, *J. Geophys. Res.*, *95*(D5), 5587-5595.

- [rogers2000] Rodgers, C.D. (2000), Inverse methods for atmospheric sounding. Theory and practice, World Scientific, Singapore.
- [smith1976] Smith, W.L., and H.M. Woolf (1976), The use of eigenvectors of statistical co-variance matrices for interpreting satellite sounding radiometer observations, *J. Atmos. Sci.*, *33*, 1127-1140.
- [smith1979] Smith, W. L., C. M. Hayden, D. C. Wark, and L. M. McMillin (1979). TIROS-N operational vertical sounder, *Bull. Amer. Meteor. Soc.*, *60*, 1177-1187.
- [smith1991] Smith, W.L. (1991), Atmospheric soundings from satellites – False expectation or the key to improved weather prediction, *Q. J. R. Meteorol. Soc.*, *117*, 267-297.
- [strow2006] Strow, L.L., S.E. Hannon, S. De-Souza Machado, H.E. Motteler, and D.C. Tobin, Validation of the Atmospheric Infrared Sounder radiative transfer algorithm, *Journal of Geo. Res.*, *111*, D09S06.
- [susskind2003] Susskind, J., C. Barnet, J. Blaisdell (2003), Retrieval of atmospheric and surface parameters from AIRS/AMSU/HSB data in the presence of clouds, *IEEE Trans. Geosci. Remote Sens.*, *41*, 390-409.
- [susskind2006] Susskind, J., C. Barnet, J. Blaisdell, L. Iredell, F. Keita, L. Kouvaris, G. Molnar, and Moustafa Chahine (2006), Accuracy of geophysical parameters derived from Atmospheric Infrared Sounder/Advanced Microwave Sounding Unit as a function of fractional cloud cover, *J. Geophys. Res.*, *111*, D09S17.
- [toohey2007] Toohey M. and K. Strong (2007), Estimating biases and error variances through the comparison of coincident satellite measurements, *J. Geophys. Res.*, *112*, D13306, doi:10.1029/2006JD008192.
- [twomey1977] Twomey, S. (1977), Introduction to the Mathematics of Inversion in Remote Sensing and Indirect Measurements, Dover Publications Inc, New York.
- [wick1971] Wick, G.L. (1971), Nimbus weather satellites: Remote sounding of the atmosphere, *Science*, *172*, 1222-1223.
- [wmo1998] World Meteorological Organization (1998), Statement of Guidance Regarding How Well Satellite Capabilities meet WMO User Requirements in Several Applications Areas, Tech. Document 922, Geneva.

- [zhou2002] Zhou, D.K., W.L. Smith, J. Li, H. B. Howell, G.W. Cantwell, A.M. Larar, R.O. Knuteson, D.C. Tobin, H.E. Revercomb, and S.A. Mango (2002), Thermodynamic product retrieval methodology for NAST-I and validation, *Appl. Opt.*, *41*, 6957-6967.
- [zhou2005] Zhou D. K., W. L. Smith, X. Liu, A. M. Larar, H.-L. A. Huang, J. Li, M. J. McGill, S. A. Mango (2005), Thermodynamic and cloud parameter retrieval using infrared spectral data, *Geophys. Res. Lett.*, *32*, L15805.

$$K = 0.8; S_a = \text{Cov}(x_a - x_t) = 1.0; \text{Cov}(y_o - y_c) = 1.0$$

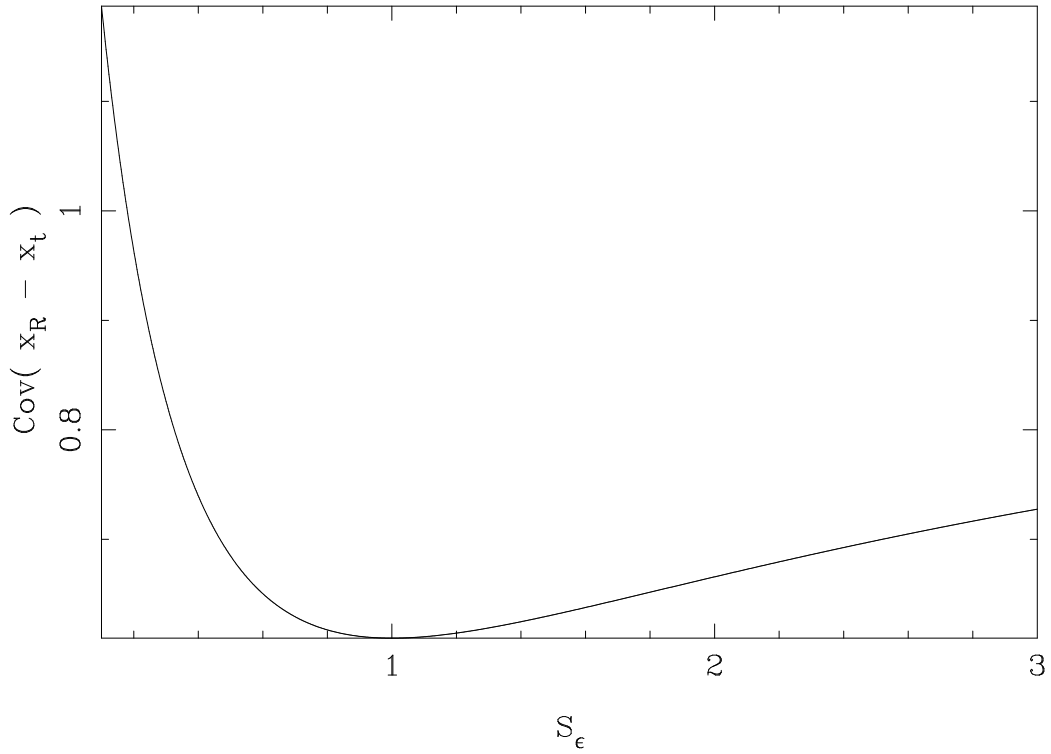


Figure 1: Retrieval error (as the covariance of the difference between the retrieved parameter and the real one, $\text{Cov}(x_R - x_v) = \overline{(x_R - x_v)^2}$) as a function of the measurement error covariance, S_ϵ , as described by Eq. 6. Other values used in this plot are $K = 0.8$; $S_a = \text{Cov}(x_a - x_v) = \overline{(x_a - x_v)^2} = 1.0$ and $\text{Cov}(y_o - y_c) = \overline{(y_o - y_c)^2} = 1.0$.

Histogram IASI Channel 3577

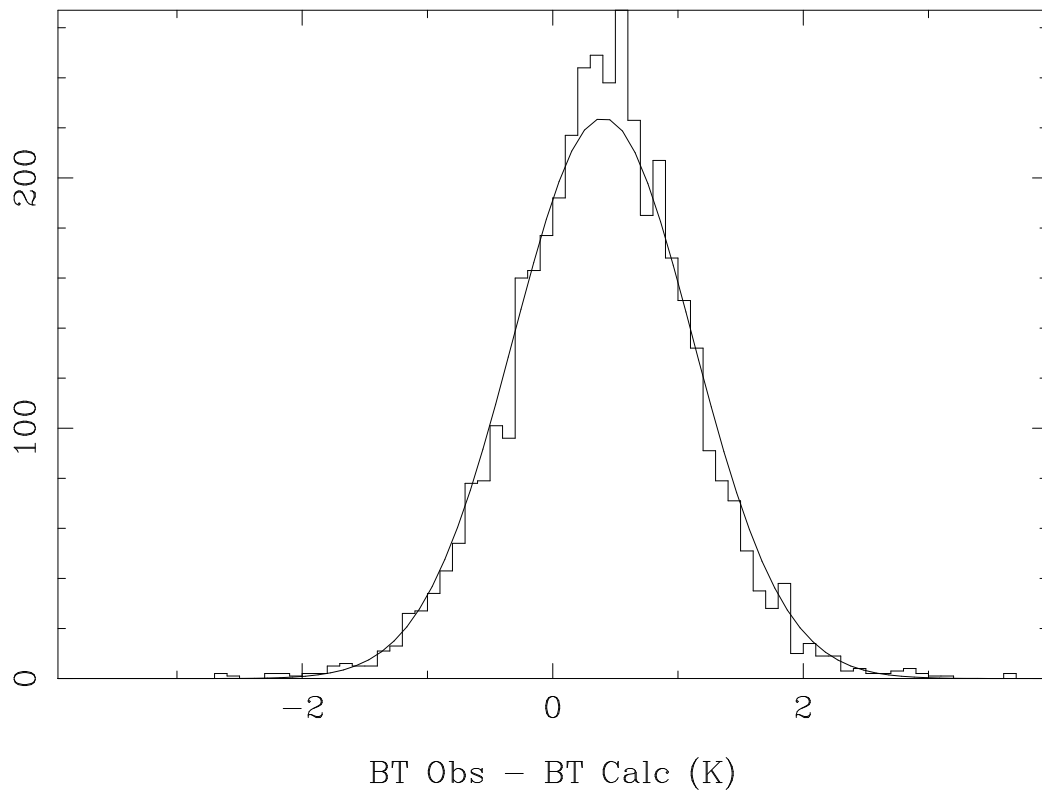


Figure 2: Histogram of brightness temperature difference between observed and calculated spectra (OBS-CALC) for IASI channel 3577 (1539 cm^{-1}). Stepwise line is the measured histogram and smooth line is the fitted Gaussian.

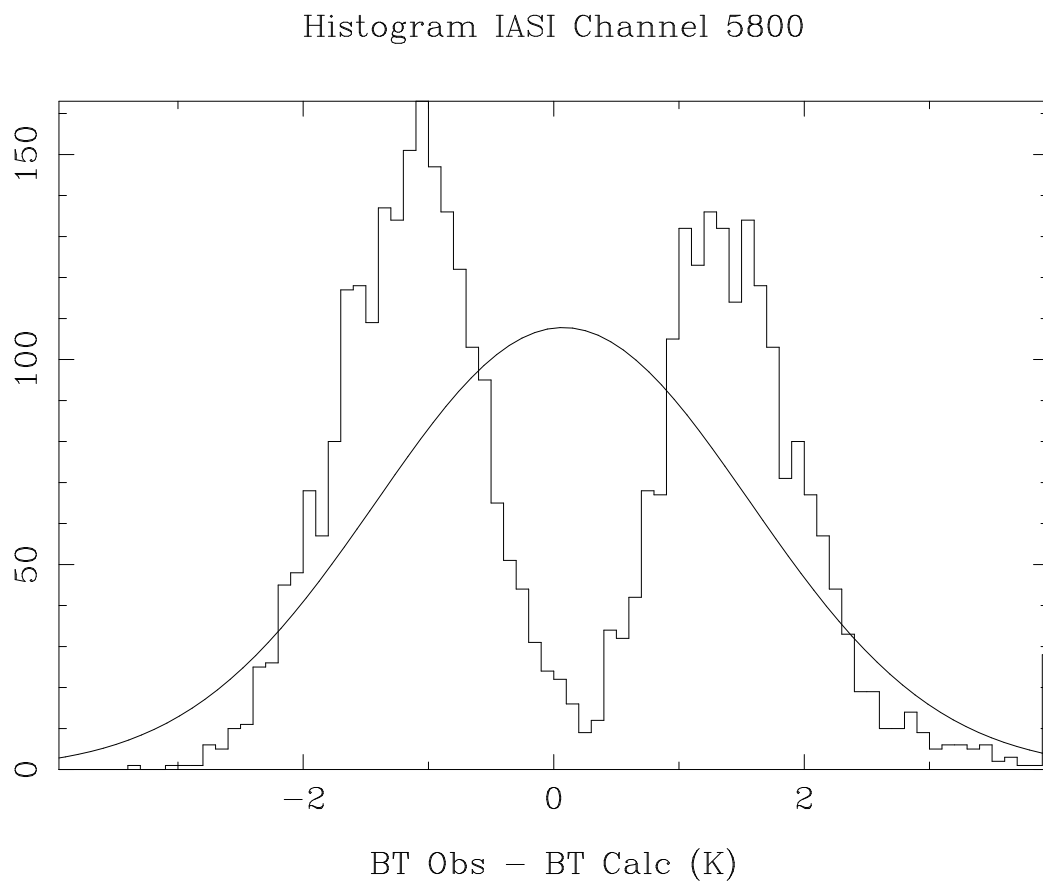


Figure 3: Histogram of brightness temperature difference between observed and calculated spectra (OBS-CALC) for IASI channel 5800 (2094.75 cm^{-1}). Stepwise line is the measured histogram and smooth line is the fitted Gaussian.

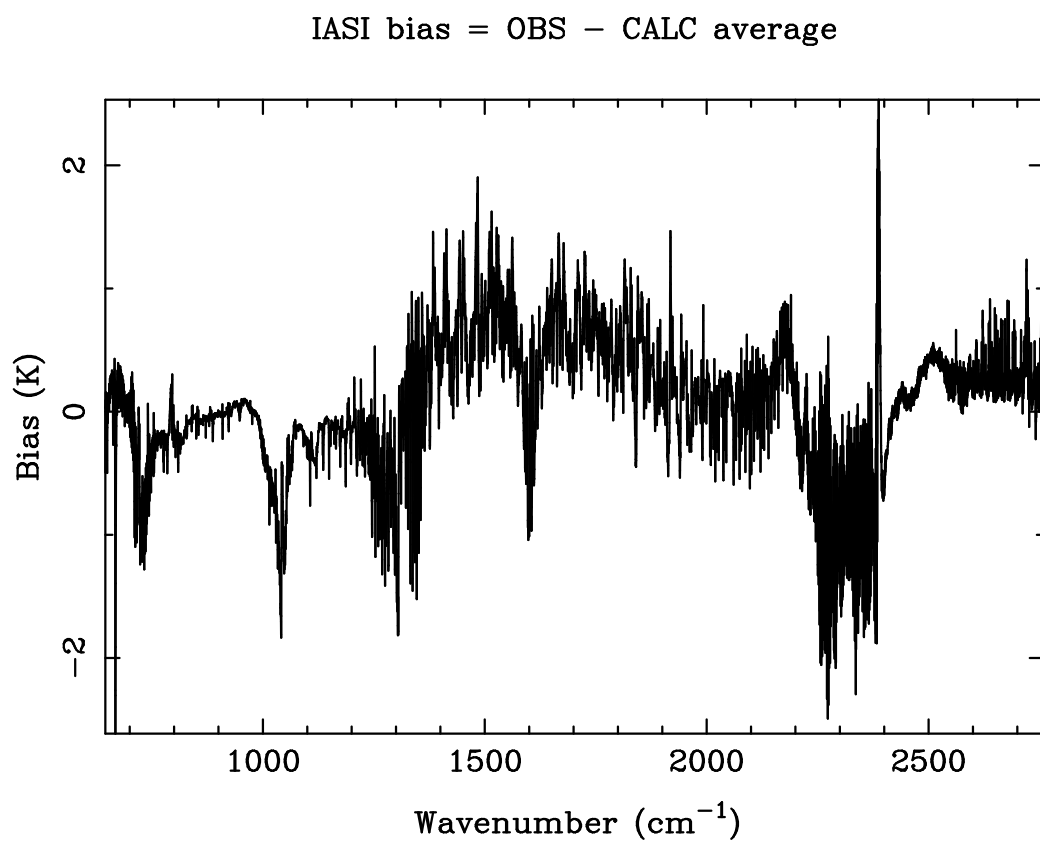


Figure 4: OBS-CALC bias: observed minus calculated (ECMWF analyses + RTIASI 4.1) brightness temperature averages for all IASI channels.

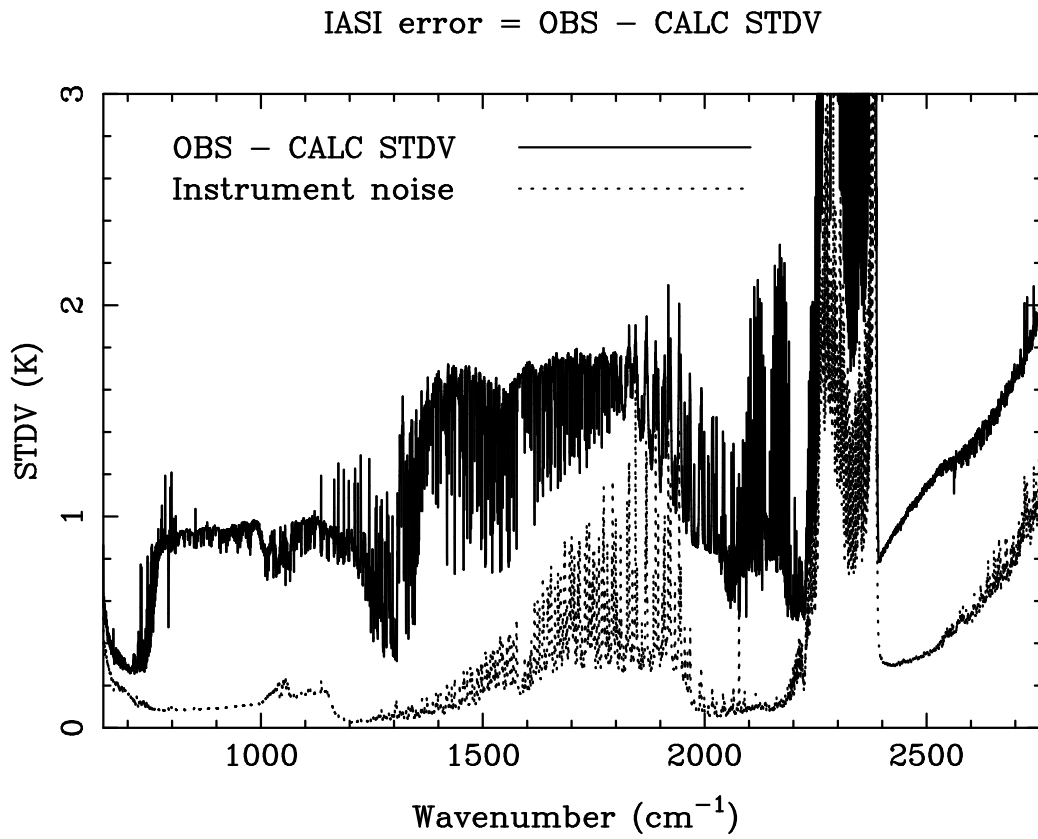


Figure 5: OBS-CALC standard deviation: observed minus calculated (ECMWF analyses + RTIASI 4.1) brightness temperature standard deviations for all IASI channels. Also shown is the instrument noise for one randomly chosen atmospheric state.

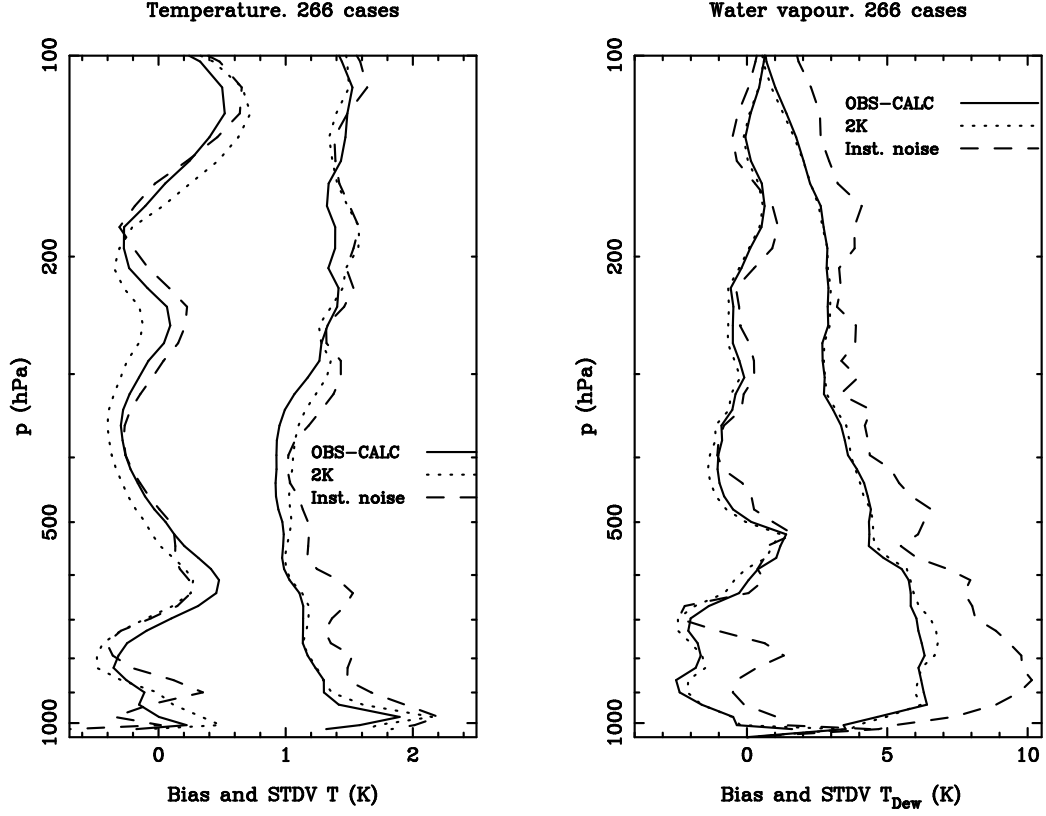


Figure 6: Bias (curves on the left of each graph) and standard deviation (curves on the right of each graph) of the retrieval statistics using the diagonal of the instrument noise, a constant of 2 K and OBS-CALC standard deviation as the error covariance matrix in the retrievals. The error covariance matrix that provides the optimal retrievals when comparing with ECMWF analyses is the OBS-CALC one as the analytical proof of Appendix A shows.

Lat=36.85° Lon=124.56°. 2007/04/18 12:23:03

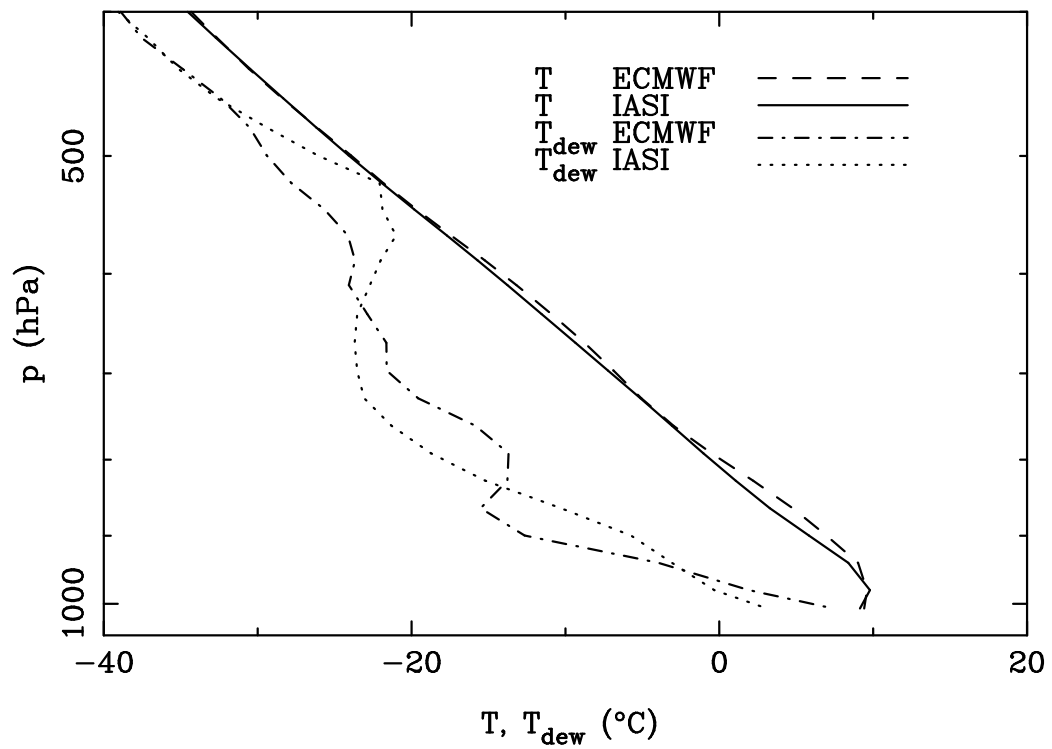


Figure 7: Typical IASI retrieval is shown together with the co-located ECMWF atmospheric profile. There is a low level inversion that is clearly retrieved.

Lat=39.29° Lon=-52.49°. 2007/04/19 00:13:11

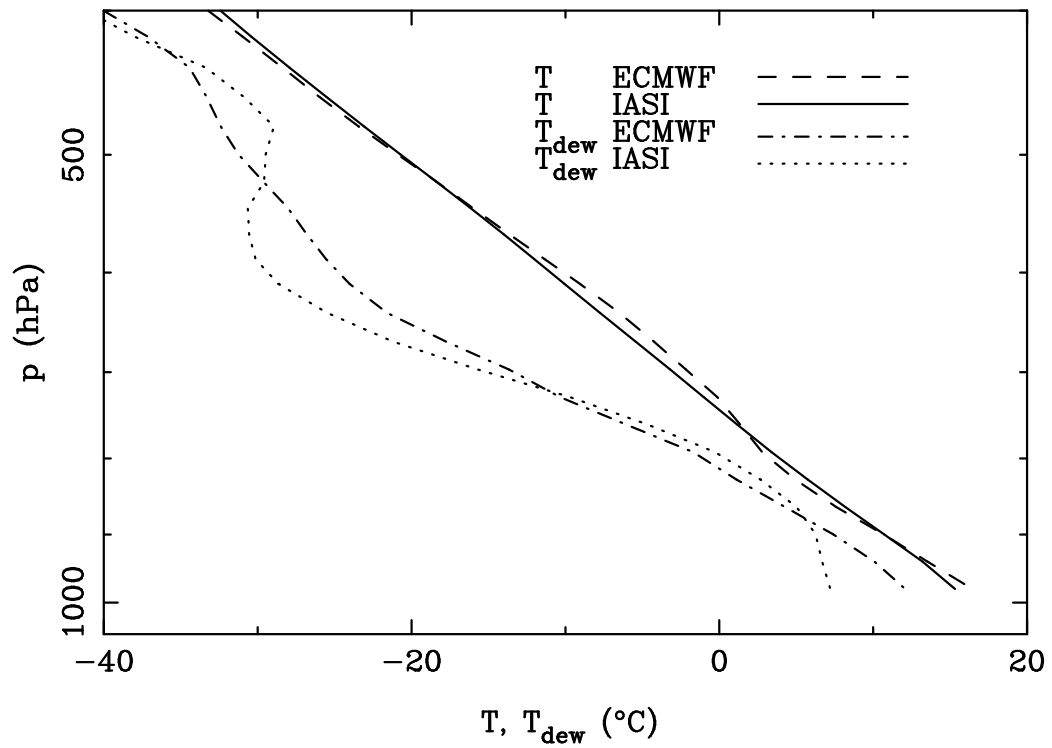


Figure 8: Typical IASI retrieval is shown together with the co-located ECMWF atmospheric profile. This one has a flatter temperature profile, which is also relatively well retrieved, as well as the humidity profile.

Lat=-45.37° Lon=146.35°. 2007/04/28 11:52:39

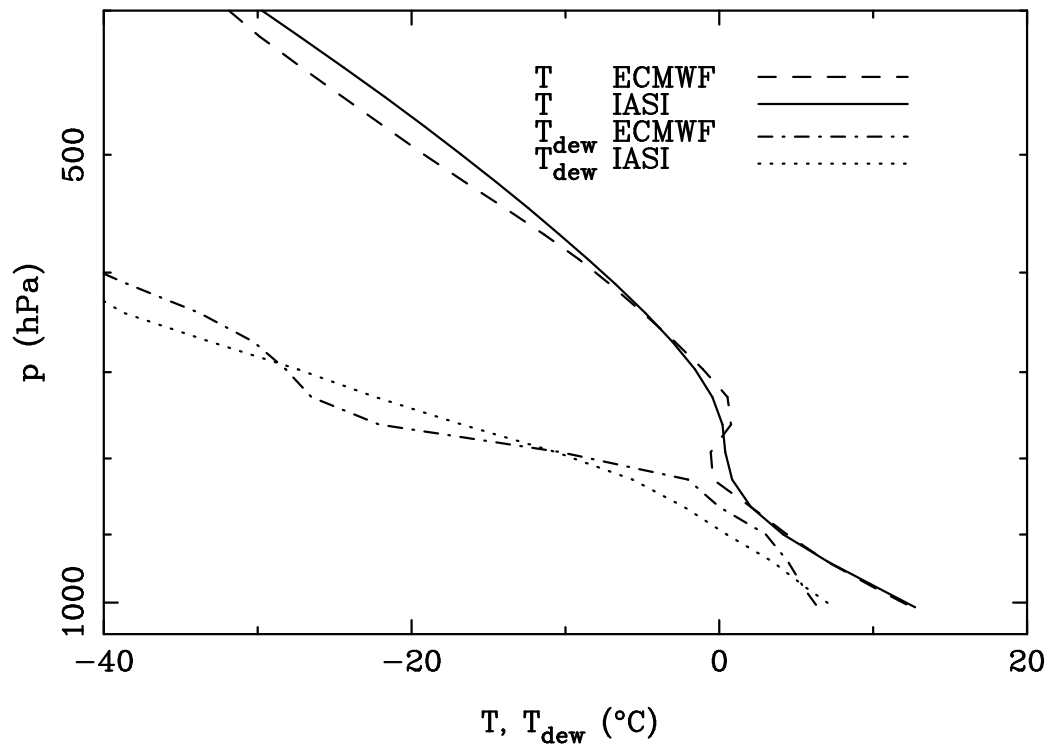


Figure 9: Typical IASI retrieval is shown together with the co-located ECMWF atmospheric profile. Here we see how a strong low level inversion is also reproduced by the retrieval even with high humidity at lower levels.

Lat=38.93° Lon=122.34°. 2007/04/28 12:16:55

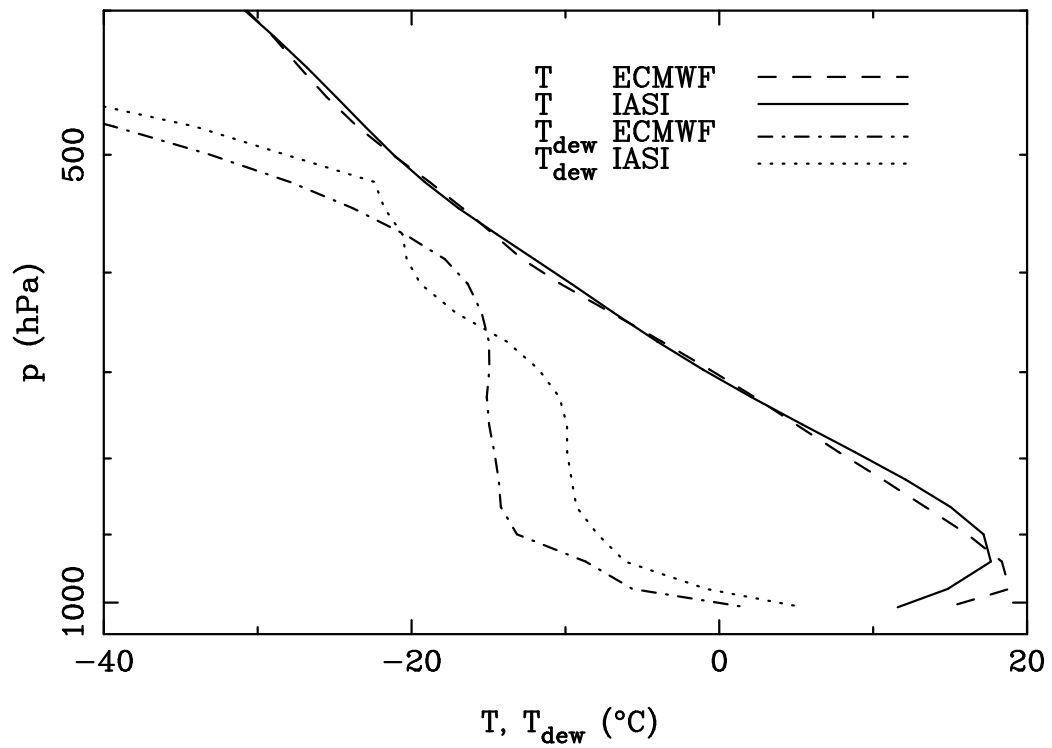


Figure 10: Typical IASI retrieval is shown together with the co-located ECMWF atmospheric profile. In this figure a humidity maximum is well reproduced, this profile also has a strong inversion near the surface.

Lindenberg 2007/06/08 19:58:01

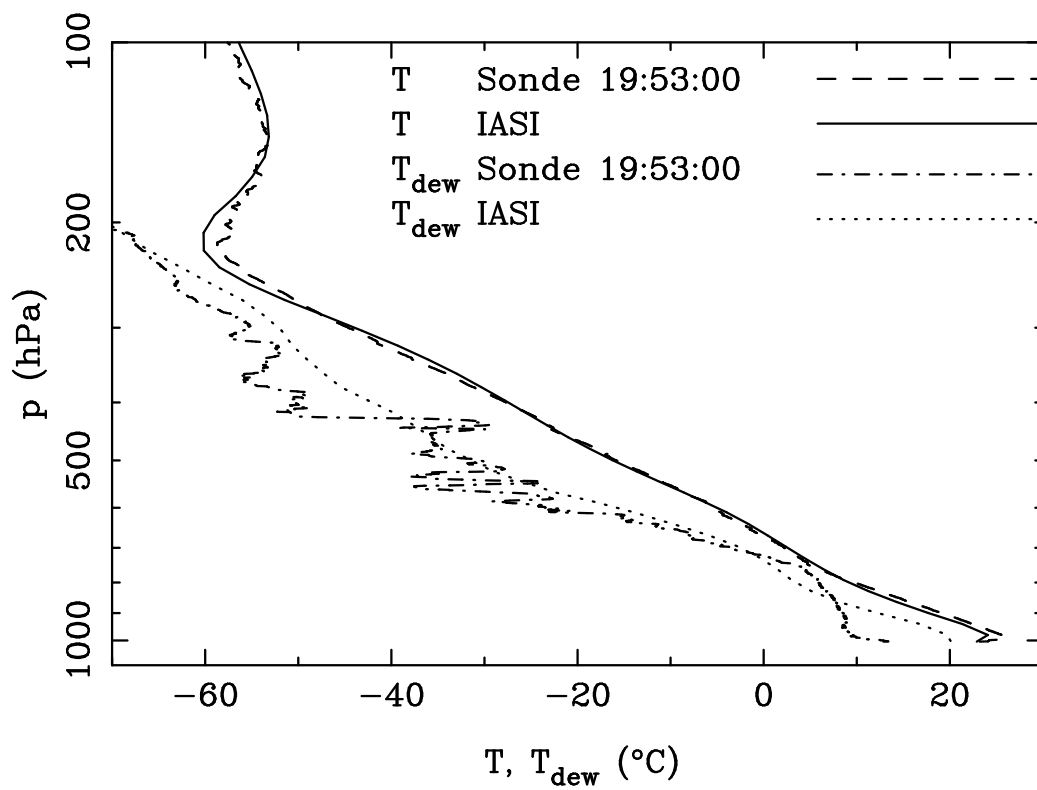


Figure 11: IASI retrieval fine tuned for ECMWF analyses compared with co-located radiosondes from Lindenberg launched five minutes before overpass time.

Lindenberg 2007/06/10 09:28:48

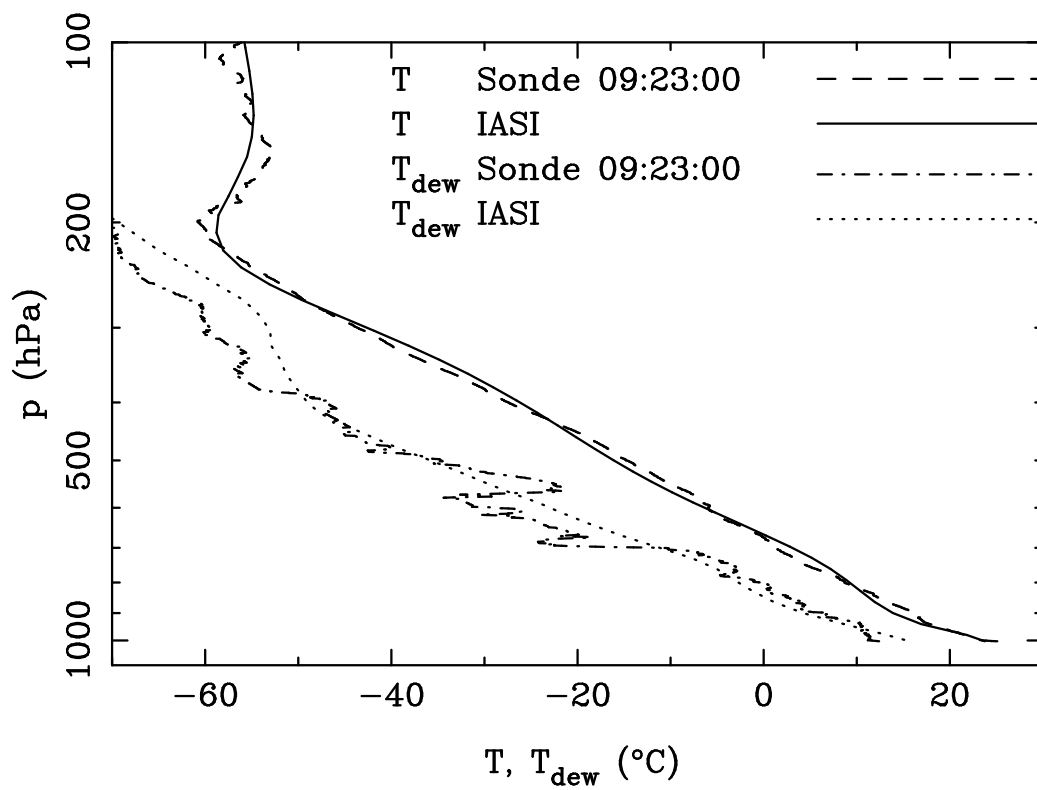


Figure 12: IASI retrieval fine tuned for ECMWF analyses compared with co-located radiosondes from Lindenberg launched five minutes before overpass time.

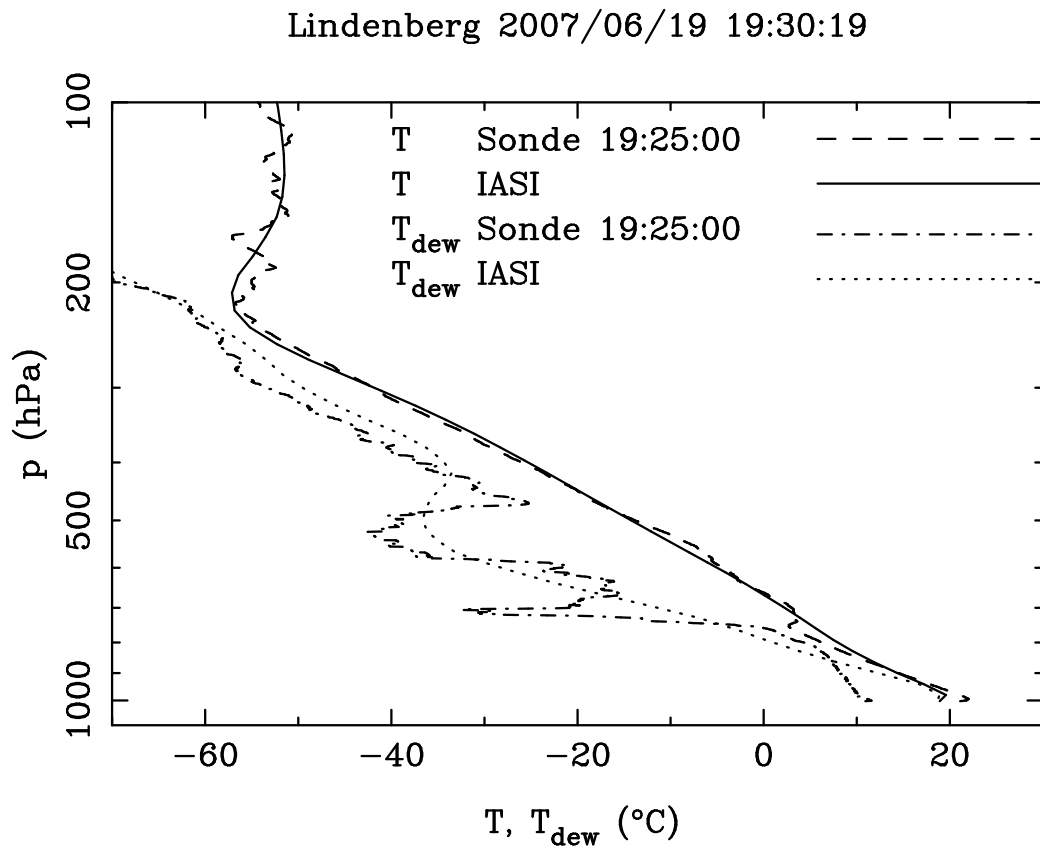


Figure 13: IASI retrieval fine tuned for ECMWF analyses compared with co-located radiosondes from Lindenberg launched five minutes before overpass time.

Lindenberg 2007/06/08 19:58:01

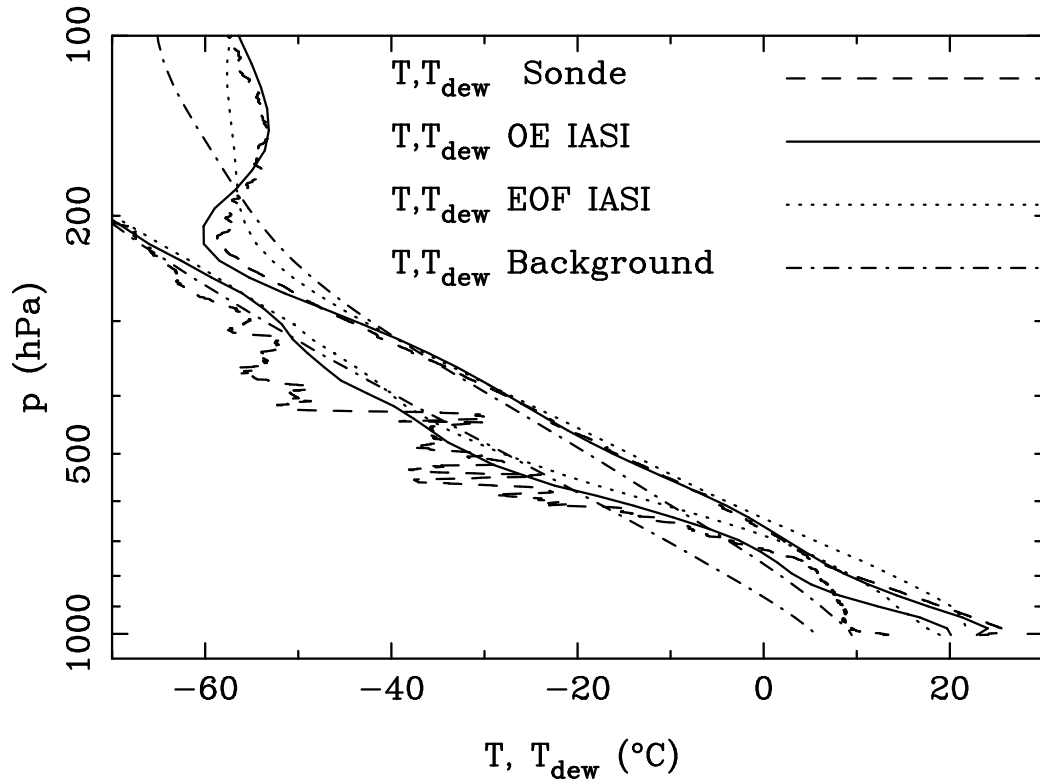


Figure 14: IASI retrieval fine tuned for ECMWF analyses compared with co-located radiosondes from Lindenberg launched five minutes before overpass time. Also added in this figure are the first guess (EOF retrieval) and background state of the optimal estimation retrieval. Lines on the left and right side correspond to dew point temperatures and temperatures respectively.

Table 1: Scene selection.

Cloud detection
$-1 \text{ K} < T(3.9 \text{ } \mu\text{m}) - T(10.8 \text{ } \mu\text{m})$ ¹ a $< 3 \text{ K}$
$T(10.8 \text{ } \mu\text{m}) > 276 \text{ K}$
$T(11.0 \text{ } \mu\text{m}) > SST$ ² b -2.2 K
$T(4.0 \text{ } \mu\text{m}) - T(11.0 \text{ } \mu\text{m}) > 12 \text{ K}$
$T(9.3 \text{ } \mu\text{m}) - T(11.0 \text{ } \mu\text{m}) < 0 \text{ K}$
$T(11.0 \text{ } \mu\text{m}) - T(12.0 \text{ } \mu\text{m}) < 1 \text{ K}$
$T(11.0 \text{ } \mu\text{m}) - T(13.6 \text{ } \mu\text{m}) > 18 \text{ K}$
Others
$ Solar \text{ zenith angle} < 80^\circ$
$ Latitude < 50^\circ$
$ Scan \text{ angle} < 15^\circ$

$T(10.8 \text{ } \mu\text{m})$, for example, is the brightness temperature of an AIRS channel that lies in that wavelength ($10.8 \text{ } \mu\text{m}$). SST is the sea surface temperature derived from ECMWF analysis.